ORIGINAL PAPER

Characteristics of partially pregelatinized sago starch from Bangka, Riau, and Papua extruded using twin-screw extruder

Sabirin[1,3] · Azis Boing Sitanggang[2] · Slamet Budijanto[2] · Mardonius Budi Kusarpoko[3] · Abdullah Darussalam[3] · Ahmad Safrudin Purwoto[3] · Yanuar Sigit Pramana[3]

Abstract

Sago starch from Bangka, Riau, and Papua could be increased in added value through the extrusion process without a die. This study aims to explore the physicochemical properties of sago starch classified based on its origin in Indonesia, namely Bangka, Riau, and Papua, including the same properties of its extruded product, namely partially pregelatinized sago starch (PPSS), for the selection of sago was best carried out process optimization. Native sago starches were extruded using a twin-screw extruder (TSE) with a moisture content of 41%, barrel temperature for zone 1–4 at (40 °C, 81 °C, 81 °C, and 81 °C) respectively, screw speed at 390 rpm, and without a die. Physicochemical properties such as degree of gelatinization (DG) and other properties were analyzed. DG of native sago starch from Bangka, Riau, and Papua were 14.27%, 19.00%, and 13.03%, respectively. Values of DG were significantly increased after the modification process using extrusion treatment into PPSS, which PPSS of Bangka, Riau, and Papua had DG of 48.91%, 39.82%, and 37.80%, respectively. Pasting properties, thermal properties, water absorption index (WAI), water solubility index (WSI), swelling power (SP), gel properties, viscosity, starch content, amylose, proximate composition, structural morphology, crystallinity, pH, bulk density (BD), degree of whiteness (DW), and birefringence were observed. PPSS of Sago Bangka has better characteristics in properties of DG, WSI, WAI, SP, DW, viscosity, gel strength, and adhesiveness, so it can be used as a binder in processed foods.

Keywords Extrusion · Degree of gelatinization · Partially pregelatinized · Sago starch

Introduction

Partially pregelatinized starch plays a very important role in Indonesian agroindustry, especially in the food agroindustry. Unfortunately, most (95%) of modified starch, or 9896 tons, were imported, including pregelatinized starch, based on data from the Central Bureau of Statistics. To increase the added value of native starch, which was available in abundance, Indonesia continuously developed modified starch technologies, including partially pregelatinized starch from various starch sources, such as Sago (*Metroxylon sagu*).

Globally, Indonesia was the biggest sago starch producer. Based on data from the Ministry of Agriculture, sago production in Indonesia reached 697,533 tons per

✉ Azis Boing Sitanggang
boing.lipan@apps.ipb.ac.id

Sabirin
sabi001@brin.go.id

Slamet Budijanto
slametbu@apps.ipb.ac.id

Mardonius Budi Kusarpoko
mard001@brin.go.id

Abdullah Darussalam
abdu023@brin.go.id

Ahmad Safrudin Purwoto
ahma001@brin.go.id

Yanuar Sigit Pramana
yanu008@brin.go.id

[1] Study Program of Food Science, Graduate School of IPB University (Bogor Agricultural University), Bogor 16680, Jawa Barat, Indonesia

[2] Department of Food Science and Technology, Faculty of Agriculture Technology (Bogor Agricultural University), Bogor 16680, Jawa Barat, Indonesia

[3] Research Center for Agroindustry, National Research and Innovation Agency, Cibinong 16911, Jawa Barat, Indonesia

year. There were many centers of sago production area, including Bangka, Riau, and Papua provinces. Bangka was an archipelago province located in the southern part of Sumatera Island. Its production of sago starch was around 12,000 tons per year. This amount contributes 1.73% of the total national sago production. Riau was in the central part of the island of Sumatra and was crossed by the equator. Production of sago starch was around 265.830 tons per year. This amount contributes 38.11% of the total national sago production. While Papua was in the Eastern part of Indonesia, production of sago starch was around 270,800 tons per year. This amount contributes 38.88% of the total national sago production. The differences in the agroecological zones were thought to bring about differences in the characteristics of the native starch produced and affect the characteristics of the modified starch obtained.

There have been various studies on the functional properties of sago, such as comprehensive research to elucidate the physicochemical and structural properties of sago starch [1]. Resistant starch type III (RS3) was produced from different sections, the top and bottom part of *Metroxylon sagu* palm at different growth stages, namely, Plawei Manit, Bubul, and Angau Muda, sago starch was subjected to two cycles of autoclaving, debranching by pullulanase, and cooling [2]. Polyvinyl alcohol was blended with sago starch films in the presence of glycerol as a plasticizer. Tensile test results revealed that films without starch have higher tensile strength than films with starch [3]. Extruding sago starch in an extrusion machine was predicted to produce partially pregelatinized sago starch (PPSS) with specific properties. One of the most significant changes due to extrusion-based modification was the increase of degree of gelatinization (DG). Sago starch granules were fused into a coarse mass after extrusion cooking, exemplifying gelatinization [4]. The increase in the DG enables the PPSS to have adhesiveness, which was useful for dough formation before the dough was cooked and gives the processed food products a softer texture. Mixing PPSS and native starch was expected to improve the quality of starch so that the dough would be easier to form. PPSS was expected to replace the function of sodium alginate. Generally, the material commonly used as a binder was sodium alginate with low viscosity (0.1–1 poise) and high viscosity (8–20 poise); for low viscosity, alginate solution has a concentration of 0.5–5%, and for high viscosity, the concentration was 5–11% [5]. Therefore, the purpose of this study was to explore the physicochemical properties of sago starch classified by its origin in Indonesia, namely Bangka, Riau, and Papua, including the same properties of its extruded product, namely partially pregelatinized sago starch (PPSS) with an increased degree of gelatinization (DG). These represent the industrial-scaled sago extraction facilities in Indonesia.

Materials and methods

Materials

Three different sago starches, i.e., Bangka sago starch (Sago 1), Riau sago starch (Sago 2), and Papua sago starch (Sago 3) were used in this experiment. Sago 1, labeled as Rumbia, was produced by PT Bangka Asindo Agri (PT BAA) from Sungai Liat-Bangka; Sago 2, labeled as Cheetah, was produced by Koperasi Harmonis from Selat Panjang; and Sago 3, labeled as Sapapua, was produced by PT Austindo Nusantara Jaya Agri Papua Barat Tbk. (PT ANJAP).

Production of PPSS

Sago starch 1, 2, and 3 were extruded under the moisture content of 41%, and barrel temperatures of zones 1 to 4 were set at 40 °C, 81 °C, 81 °C, and 81 °C, respectively. Screw speed was set at 390 rpm. PPSS products for Sago 1, 2, and 3 were labeled PPSS 1, PPSS2, and PPSS 3. The extrusion products were dried using sun drying until they reached a moisture content of 12%. Extruded sago flours were stored in air-tight plastic bags at 25 °C until further analyses.

Proximate composition

Moisture, lipid, protein, ash, and total starch content were determined using AOAC methods 925.10, 920.85, 992.15, 923.03, and 996.11, respectively [6]. Total amylose content was measured by following Hoover and Ratnayake [7], a modification from the work of Mcgrance [8].

Surface morphology observation

The surface morphology and particle size were determined during scanning electron microscopy analysis using Thermoscientific, Quattro S type, The Netherlands with ×2000 magnification was utilized. Elemental composition of synthesized samples was determined during FE-SEM analysis using a Bruker EDS Device. A thin gold layer first covered the surface of the samples. After that, the sample was placed into the FE-SEM and the surface image using a Secondary Electron (SE) detector with a working distance (WD) of 8–9 mm and HV 20 kV.

Starch crystallinity

The spectrum pattern and the crystallinity of materials were analyzed using XRD (Panalytical, x'pert3 powder, Malvern,

The Netherlands). The measurement was performed using a tube with 2θ: 5–80° at 40 kV, 20 mA, and a speed of 2°/min.

Pasting properties

Brabender viscograph-E (GmbH & Co. KG, Germany) was utilized to examine the pasting properties. The experiment was undertaken by performing the heating and cooling cycles with constant stirring (75 rpm) to the 500 g of the sample. The sample was heated from 50 to 93 °C, and the achieved temperature was maintained for 15 min. After that, the temperature was decreased to 50 °C, which was then maintained for 10 min. This process was performed once, and the result was presented as a viscosity profile.

Thermal properties

The thermal properties of starch samples were measured by DSC (NETZSCH DSC 214 Polyma DSC21400A-0710-L. NETZSCH-Gerätebau GmbH Wittelsbacherstraße 42 95100 Selb, Germany). Starch sample (~ 7 mg, dry basis). The pan was sealed, allowed to equilibrate at 25 °C for 2 h, and heated from 20 to 200 °C (10 °C/min) without adding water.

pH determination

The pH analysis was undertaken using a magnetic stirrer by mixing 0.1 g of the sample and 100 mL of distilled water in the beaker glass. On the other hand, the suspension was measured using a calibrated pH meter (Horiba, Japan) at room temperature. The result shown on the pH meter screen was then recorded.

Bulk density (BD)

The method used to analyze the bulk density (BD) was by following Wang and Kinsella [9]. A sample of as many as 10 mL was initially weighed before being placed into a pycnometer chamber (Pyrex-USA) with the same volume. Then, packing was performed by gently tapping the pycnometer above its bench until it reached a constant volume. BD was a ratio obtained by dividing the weight (g) of the sample by its volume (mL).

$$BD = \frac{Weight\,(g)}{Volume\,(mL)} \tag{1}$$

Degree of whiteness (DW) and viscosity

Digital Portable Whiteness Meter (Zhejiang Top Cloud-Agri Technology Co., Ltd, China) was utilized to measure the whiteness of the sample, while viscosity was analyzed using Viscotester Rion, VT-04F. To determine the viscosity, a sample was placed between the outer wall of the rotor and the wall inside the cup suitable for the rotor. In the measurement process, the test liquid containing about 15% of the sample (w/v) was put into the cup. The tool was then turned on after the rotor was placed in the center of the cup. After that, the result shown on the instrument scales was then recorded.

Degree of gelatinization (DG)

The degree of gelatinization (DG) was measured by Wootton et al. [10] by utilizing a Spectrophotometer pharo 300, KGaA 64271 Darmstadt, Germany, with a wavelength of 620 nm. Sample preparation for the gelatinized starch sample stock was as follows: 0.25 g of sample, which passed 40 mesh, was dispersed into 23.5 mL + 1.25 mL NaOH 10 M and 24.75 mL distilled water. Sample was then homogenized for one minute. The suspension was centrifuged at room temperature for 30 min at 3500 rpm. After that, 0.5 mL supernatant + 0.5 mL HCl 0.5 M was filled with 10 mL distilled water, then vortexed and homogenized. The gelatinized starch blank (Solutions A and C) was as follows: 1 mL solution was filled with 10 mL distilled water and homogenized using a vortex. In the other set, the gelatinized starch sample (Solution B and D) was as follows: 1 mL solution was prepared, to which 0.1 mL of Iodin solution was added. Then, it was filled with 10 mL of distilled water and homogenized using a vortex. Lastly, a spectrophotometer was utilized to read the sample. The following formula was then used:

$$DG = \frac{Absorbance\ value(B - A)}{Absorbance\ value(D - C)} \times 100\% \tag{2}$$

Water absorption index and water solubility index (WAI and WSI)

WAI and WSI from the extrudate were determined by following Anderson et al. [11]. A 2.5 g (dry base) of extrudate (< 60 mesh) was dissolved in 30 mL of water at 30 °C for 30 min, followed by centrifugation at 3000 rpm for 10 min. The supernatant was separated from the gel and dried at 105 °C until it achieved the constant weight. WAI and WSI were then calculated using the following formulas:

$$WAI = \frac{Weight\ of\ water\ absorbed\,(g)}{Dry\ weight\ of\ extrudate\,(g)} \tag{3}$$

$$WSI = \frac{Weight\ of\ dry\ sediment}{Volume\ of\ supernatant} \times 100\% \tag{4}$$

Swelling power (SP)

Swelling power (SP) analysis was conducted using Leach et al. [12]. The procedure began by weighing the empty tube (W0). Then, 0.1 g of sample was placed into the tube (W1), adding 10 mL of distilled water. For 30 min, the sample was heated to 60 °C while continuously stirred before the tube was centrifuged at 2500 rpm for another 30 min. Lastly, the paste was separated and weighed (W2). The following formula was then used:

$$SP = \frac{W2 - W0\,(g)}{W1\,(g)} \tag{5}$$

Gel properties

The gel properties of PPSS were analyzed using marmalade method modification test by Wang et al. [13]. Gel strength and adhesiveness were obtained by using the Texture Analyzer (TA.XT Plus Stable Micro System Type plus100 series, producer Schroff, United Kingdom) with a cylindrical probe (P/0.5). Mode: Measure Force in Compression; Pre-Test Speed: 3.0 mm/s; Test Speed: 0.1 mm/s; Post-Test Speed: 10.0 mm/s; Distance: 2 mm; Trigger Type: Auto—10 g; Tare Mode: 200 pps; Accessory: 0.5″ Cylinder (P/0.5R), and was tested at 20 °C. Observations: After a trigger force of 10 g was attained, the probe penetrated the gel to a depth of 20 mm. During penetration, the force was shown to drop at the point where the gel breaks. After this, the resulting forces were due to continuing penetration up to the required depth. The maximum + ve force (i.e., the rupture point of the gel) was taken and recorded as 'rupture strength' (or 'rupture force'). The distance the gel penetrates before this break indicates the gel's elasticity, i.e., a short distance of penetration before the break indicates a brittle gel. In contrast, a large penetration distance before rupture indicates a more elastic gel. When the probe withdraws from the sample, the total force (area under the negative region of the curve) required to do this was measured and recorded as the adhesiveness.

Birefringence properties

Analysis of birefringence properties using the ZEISS ZEN 2 Core Polarization Microscope (Carl Zeiss Microscopy GmbH Carl-Zeiss-Promenade 10 07745 Jena, Germany).

Statistical analysis

All measurements were conducted in triplicate. The experimental data in this study were expressed as mean ± standard deviation. Statistical analyses of all data were performed using Statistical analysis using the SPSS software (version 23; SPSS Inc.; Chicago, IL, USA). Analysis of variance (ANOVA) and Duncan's multi-range test were used to determine significant differences ($p < 0.05$).

Results and discussion

Proximate composition, starch, and amylose

The starch sample was significantly different in terms of proximate composition (Table 1). The total starch content from the three sago starches was higher than 80%, showing that the sago starch was an ideal source of starch. The amylose contents from Sago starch 1 and 2 were significantly higher than that of Sago 3. Interestingly, the results were higher than that presented in the previous study which reported that the amylose content was $30.6 \pm 0.4\%$ [14] and ranging from 24 to 31% [15]. High amylose content generates susceptibility against retrogradation and enables sago starch paste to have higher elasticity [16]; these were favorable conditions to produce gelling agents and partially pregelatinized starch, which can act as a binder.

This experiment discovered that the amylose content of PPSS 1, 2, and 3 decreased from that of their native source (Table 1). The result demonstrated that the extrusion under this experiment's condition caused the decrease of amylose, which was responsible for increased swelling power. Amylose levels decrease due to increased temperature, which is thought to result in depolymerizing amylose components

Table 1 Proximate composition of sago starch and PPSS

Starch/extrudate	Moisture (%)	Ash (%)	Lipid (%)	Protein (%)	Starch (%)	Amylose (%)
Sago 1	10.17 ± 0.62^a	0.18 ± 0.07^b	0.09 ± 0.03^a	0.049 ± 0.01^a	88.67 ± 1.02^b	36.05 ± 0.20^{cd}
PPSS 1	11.50 ± 0.61^a	–	–	–	–	32.84 ± 0.05^a
Sago 2	17.48 ± 0.14^b	0.17 ± 0.03^b	0.06 ± 0.06^a	0.115 ± 0.00^a	83.98 ± 0.42^a	37.24 ± 1.59^d
PPSS 2	10.55 ± 3.14^a	–	–	–	–	35.05 ± 0.18^{bc}
Sago 3	11.09 ± 0.23^c	0.13 ± 0.01^a	0.23 ± 0.27^b	0.897 ± 0.08^b	88.67 ± 0.24^b	33.26 ± 1.98^{ab}
PPSS 3	12.03 ± 1.75^a	–	–	–	–	31.55 ± 0.16^a

Results were means ± standard deviations of triplicate analysis. Values with the different letters in the same column were significantly different ($p \leq 0.05$)

so that amylose has a low molecular weight. Similar results were previously reported [17]. The proximate of the extrusion products was considered identical to that of their initial sago starch since no other materials were added except water to control the moisture content.

Morphological characteristics

The surface morphology and elemental composition of the sago starch and PPSS particles were investigated using FE-SEM micrographs and EDX spectra. Figure 1 illustrates FE-SEM micrographs of Sago samples 1, 2, 3, and PPSS 1, 2, 3. Based on FE-SEM analysis, the morphology of starch granules from three different plant origins was identical, had a smooth surface, and was round or oval. Some particles have their ends cut off, but most are intact. This condition was likely caused by mechanical movement during starch extraction. Similar granule morphology, as found in this experiment, has also been reported in other studies [14, 15, 18, 19]. The samples came from different
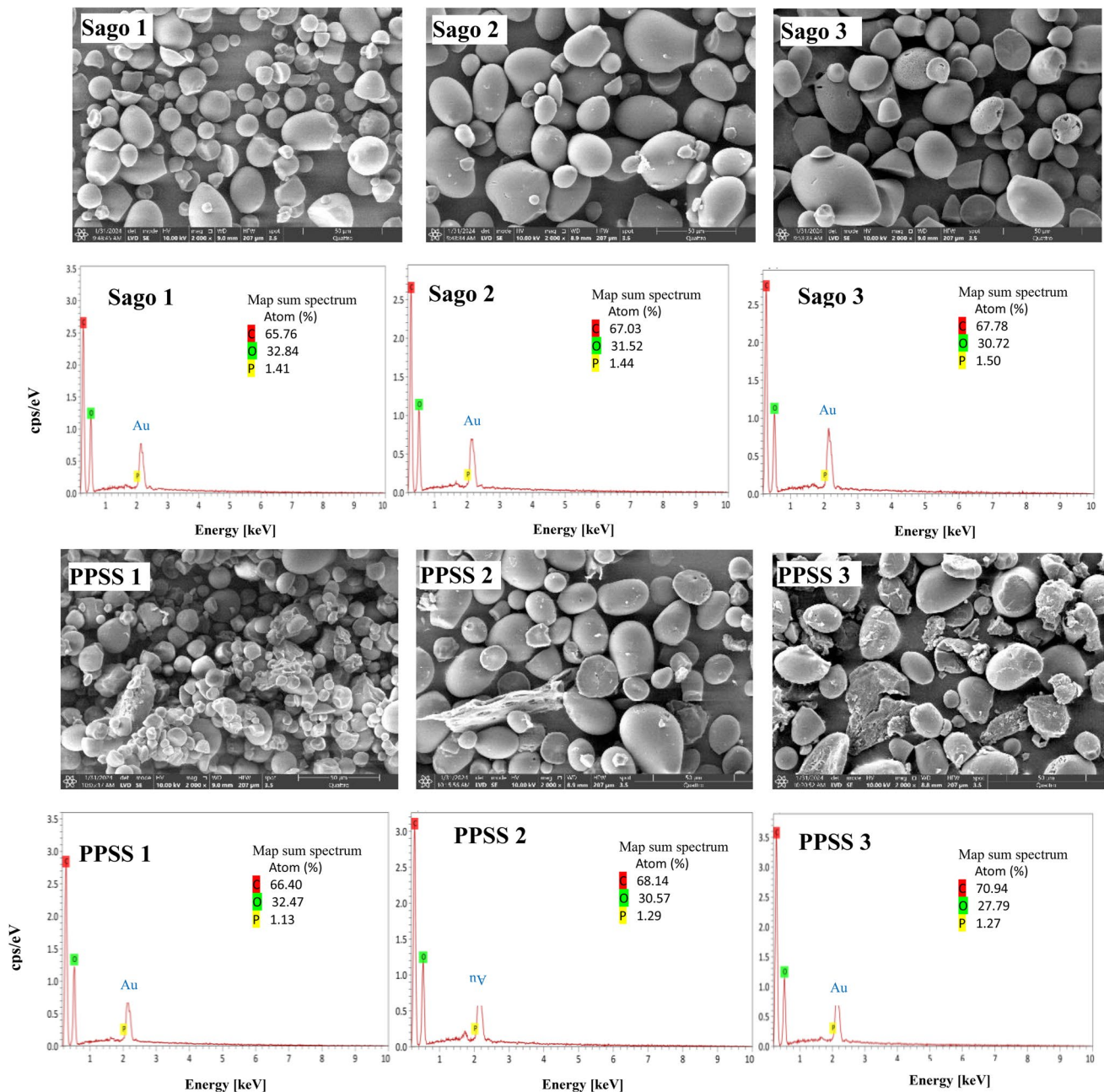

Fig. 1 FESEM micrographs and EDS spectra of Sago 1, 2, 3, and PPSS 1, 2, 3 samples

plants, and the morphology of the 3 sago palms was significantly different from each other. It can be seen that there are porous granules in Sago 3. From the FE-SEM analysis, it can be clearly noticed that the sizes of particles of Sago 1 (3.455–32.83 μm), Sago 2 (5.186–33.04 μm), and Sago 3 (5.93–32.04 μm). The observation results were that the size of sago starch granules from Malaysia was 5–20 μm for small granules, while large sago starch granules were 20–40 μm in size [20].

The FE-SEM image of PPSS reveals that the PPSS morphology has a smaller particle size after extrusion than sago starch. Some starch granules have been gelatinized, and some have not been gelatinized. Starch granules from PPSS 1 that have not been gelatinized have a particle size of (3.239–16.08 μm), PPSS 2 particle size (1.95–23.82 μm), and PPSS 3 (4.46–23.02 μm) forms starch granules that stick together, irregularly, loss of surface smoothness and the appearance of more irregular shapes. Water diffuses into the starch granules, which receive more heat during heating. As a result, the starch granules swell, and the crystallites melt, causing some of the granules to gelatinize and causing changes in the shape and size of the starch granules to become larger [21, 22].

EDS analysis shows that the carbon content of PPSS increases because the oxygen and phosphorus content decreases compared to sago starch; this was probably the extrusion heating causing hydrogen bonds with oxygen and phosphorus was a weak bond that was easily separated from the starch granules, while carbon forms strong bonds with most other elements. This was because the small atomic size of carbon enables its nucleus to hold on strongly to the shared pairs of electrons. Besides the phosphorus, oxygen, and carbon, the gold peak corresponds to the gold grid used for FESEM sample preparation—similar results from previous studies [23]. Figure 1 shows that PPSS 1, 2, and 3 have irregular degrees of shape and surface roughness. Our results are similar to those reported previously [24], where starch granule morphological transformation became the indication that the starch was partially pregelatinized.

Starch crystallinity

The crystal structure of starch could be classified into types A–C according to their amylopectin side chain clusters and double helix formations [25]. Sago starch had a C-type diffraction pattern [18, 26, 27]. The C-type pattern is a mixture of A- and B-crystalline types [28]. The peak at a 2θ value of 17° is a feature of the B-type crystal, while the peak at 23° is characteristic of the A-type crystal [29]. Based on the XRD spectrum (Fig. 2), the diffraction peak for sago 1 was at diffraction angle (°2θ) of 15.04° 17.09° 17.89°, and 22.80° for Sago 2, the peak was at 2θ of 15.04°, 17.01°, 18.06°, and 22.86° while the peak for Sago 3 was at 2θ of
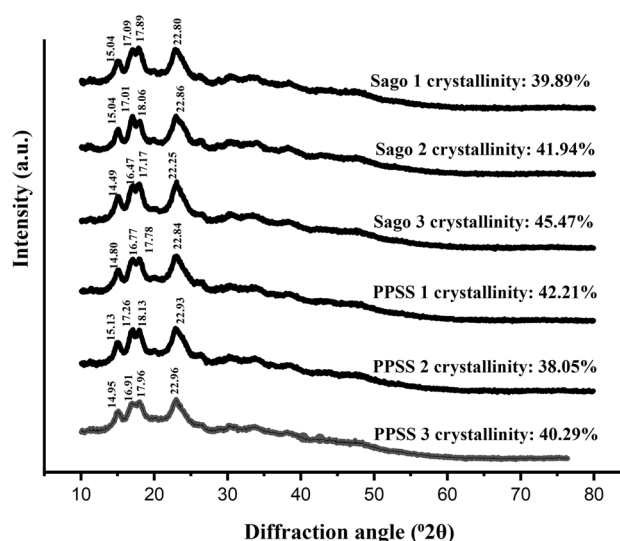

Fig. 2 X-ray diffraction patterns (XRD) of Sago 1, 2, 3, and PPSS 1, 2, 3

14.49°, 16.47°, 17.17°, and 22.25°. As for the PPSS, the diffraction peak was at 2θ of 14.80°, 16.77°, 17.78°, and 22.84° for PPSS 1 and 2θ of 15.13°, 17.26°, 18.13°, and 22.93° for PPSS 2. Lastly, the diffraction peak for PPSS 3 was at 2θ of 14.95°, 16.91°, 17.96°, and 22.96°, which indicated that PPSS had a type-C crystal pattern. In this study, extrusion products' crystallinity degree (crystal peak/total area) was lower than their respective sago starch. As discovered in the experiment, the crystallinity degree of sago 1 was 39.89%, lower than that of PPSS 1, which was 42.21%. There was a possible cause that amylopectin and amylose starch molecules ruptured into small molecules, and then small molecules reacted to form larger molecules so that crystallinity increased. The crystallinity degree of Sago 2 (41.94%) and Sago 3 (45.47%) were also higher compared to their respective PPSS 2 (38.05%) and PPSS 3 (40.29%). The extrusion process under these conditions causes some crystals to turn amorphous. The extrusion process also causes some of the crystal components to increase.

Pasting properties

Pasting properties (gelatinization profile) in this paper were reported in Table 2 and Fig. 3. These pasting properties indicated more organized double helix coordination in the amylopectin [1]. In this study, Sago 1 and 2 had high peak viscosities (PV), breakdowns, and setbacks during heating. This result was the same as the previous study's statement that native sago starch undergoes high breakdown during heating and shearing and exhibits relatively high retrogradation, forming a long cohesive gel with increased syneresis [30]. Sago 3, with low amylose

Table 2 Pasting properties of Sago 1, 2, 3, and PPSS 1, 2, 3

Starch/PPSS	Pasting parameters													
	BoG		PV	PT	SoHP		SoCP		EoCP		EoFHP		BV	SV
	BU	°C	BU	°C	BU	°C	BU	°C	BU	°C	BU	°C	BU	°C
Sago 1	11	69.9	704	77.2	433	92.8	271	92.9	507	51.8	506	50	433	236
PPSS1	12	68.5	420	76.2	314	92.5	208	93.0	357	51.2	342	51	212	149
Sago 2	12	71.3	520	75.6	384	92.8	233	93.1	421	52.3	420	50	287	188
PPSS 2	12	72.7	422	76.8	329	93.1	208	93.1	385	51.9	376	50	214	177
Sago 3	11	74.5	23	76.4	10	92.8	8	93.1	14	51.1	23	50	15	6
PPSS 3	0	45.1	8	76.2	6	92.8	4	93.1	9	50.8	9	50	4	5

BoG beginning of gelatinization; *PV* peak viscosity; *PT* pasting temperature; *SoHP* start of holding period; *SoCP* start of cooling period; *EoCP* end of cooling period; *EoFHP* end of final holding period; *BV (breakdown viscosity)* PV-SoCP; *SV (setback viscosity)* EoCP-SoCP
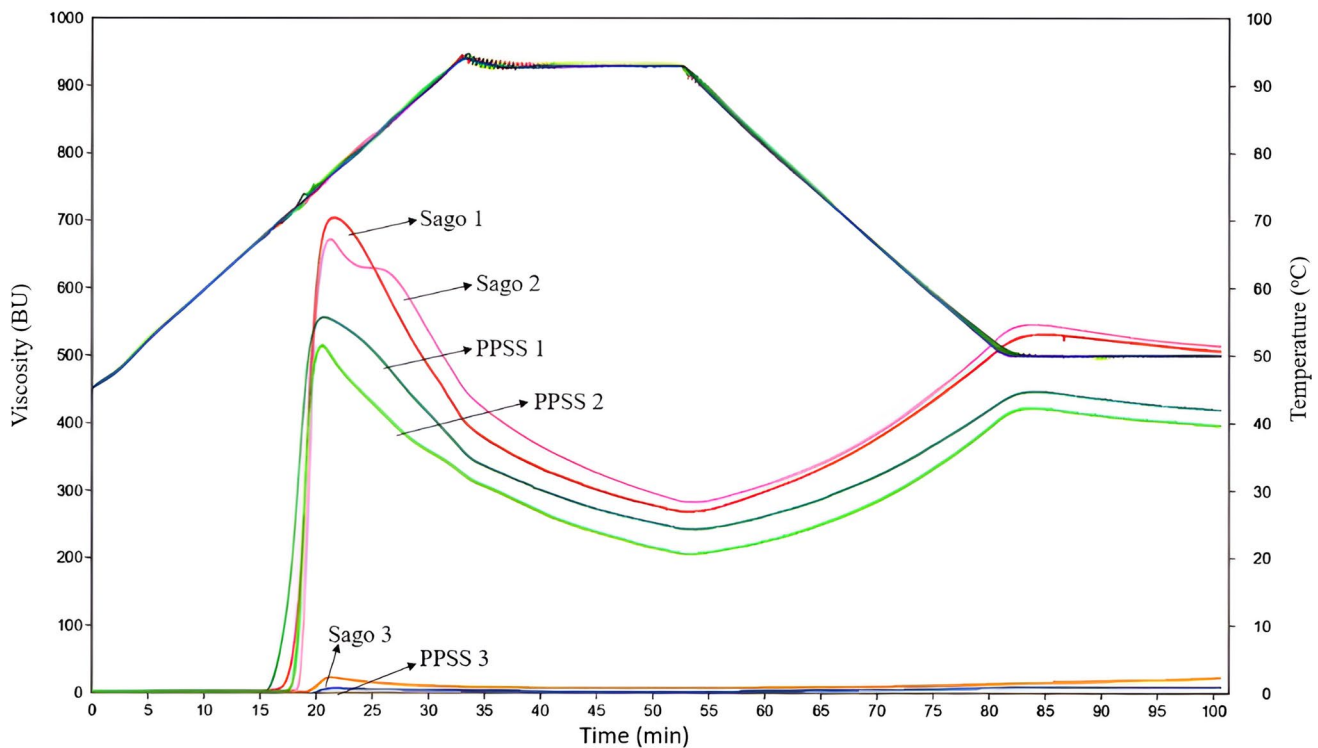

Fig. 3 Gelatinization profile of Sago 1, 2, 3, and PPSS 1, 2, 3

content, had the lowest PV. It might happen because amylose can limit the swelling of starch granules and form a complex that does not dissolve during the gelatinization process [31]. The PV of Sago 3 and PPSS 3 were significantly lower than that of Sago 1 and PPSS 1 with Sago 2 and PPSS 2, possibly due to part to the porous Sago 3 granules shown in Fig. 1c. In the current experiment, sago starch from the three different botanical origins had higher setbacks than their respective PPSS, which indicated that PPSS had higher cooling stability and gel-forming/retrogradation. Differences in genotype generate additional PV for both sago starch and its extrusion product.

Thermal properties

The sample quantified its thermal properties in terms of gelatinization by using DSC without adding water. Enthalpy (ΔHg) and heat flow of Sago 1, 2, 3, and PPSS 1, 2, 3 were presented in Table 3, and DSC thermograms were in Fig. 4. ΔHg and heat flow of Sago 1 were lower than PPSS 1, Sago 2 was higher than PPSS 2, and Sago 3 was higher than PPSS 3. The higher peak gelatinization temperature of Sago 1 indicates that melting sago crystals were more stable than PPSS 1. However, enthalpy PPSS 1 becomes higher than Sago 1; this has been proven by XRD analysis, which has

Table 3 The thermal properties of Sago (1, 2, and 3) and PPSS (1, 2, and 3) were measured using DSC at the level of heating 10 °C/min

Starch/extrudate	To (°C)	Tp (°C)	Te (°C)	ΔH_g (J/g)	HF (mW/mg)
Sago 1	29.6	91.0	172.9	341.6	0.8760
PPSS 1	27.9	83.1	171.0	362.7	0.9676
Sago 2	28.3	94.3	170.9	424.3	1.1450
PPSS 2	31.0	100.7	184.7	369.3	0.9153
Sago 3	29.4	89.6	171.1	358.2	0.9204
PPSS 3	29.9	90.1	195.9	308.3	0.7404

HF heat flow; *To* onset temperature; *Tp* peak temperature; *Te* endset temperature

been explained in the discussion of crystallinity. The higher peak gelatinization temperature of PPSS 2 and 3 indicates that melting sago crystals were more stable than Sago 2 and 3. The variation in ΔHg represents the difference in bond strength between the double helixes that make up the amylopectin crystals. This results in the alignment of different hydrogen bonds in starch molecules [32]. Therefore, higher ΔHg and heat flow lead to higher granule stability visible on Sago 2 and 3. Molecular interactions (mainly hydrogen bonds between starch chains) in PPSS involve amylose gelation, i.e., gel tissue formation and recrystallization of amylopectin [33]. The lower enthalpy value was thought to be due to its weak crystallinity [1].

pH, BD, DW, viscosity, DG, WSI, WAI, and SP

pH, BD, DW viscosity, DG, WSI, WAI, and SP properties in this paper were reported in Table 4. In the current study, the pH of Sago 3 was significantly lower than that of Sago 1 and 2. The water used in the extraction process study might be responsible for the low value of the sago starch pH. The pH value of PPSS 1, 2, and 3 was significantly higher after 41% water was added during the extraction process. Among all sagos and PPSS in this work, sago 1 and PPSS 1 had the highest pH values within their respective group.

Compared to their sago starch, the three PPSSs exhibited lower BD. The extrusion process transformed some crystalline particles into amorphous ones responsible for the looser starch granules. In rice flour extrusion, the moisture content of the materials was significant to the various properties of extrudates, where the increase of materials' moisture content affected the decrease of BD [34]. The BD of Sago 1 and 2 was not significantly different from its PPSS, while the BD of PPSS 3 was considerably lower than that of Sago 3.

The extrusion process also influenced the decrease in DW. There were significant differences in the DW of sago starch and their PPSS in this study, in which PPSS 2 exhibited the lowest DW. The poor extraction and extrusion might

be responsible for this phenomenon, as the said processes caused the polyphenol to stay in the Sago 2. These polyphenols were accountable for the starch's light brown color [35]. Consequently, oxidation happened due to heating, which then caused PPSS 2 to have a duller color compared to other PPSS. PPSS viscosity increased after extrusion. Using water during heating allowed the swollen starch granules to be gelatinized. During drying, the trapped water was released from the starch granules, creating hollow areas where cold water could be easily absorbed. Study about extruded breadfruit flour and its potential as a gel-forming agent in food protein/starch systems [36]. The viscosity of PPSS 1 was higher than PPSS 2 and 3, which indicates that PPSS 1 is more soluble in cold water.

The DG of Sago 1, 2, and 3 increased when they transformed into their PPSS. The increase, however, did not reach a 60% value because the extrusion process was performed with a high screw speed (390 rpm) and without a die. These conditions were also responsible for the low residence time of the starch, which resulted in the low amount of starch being gelatinized. DG decreased as the screw speed increased [37]. Study that moisture content indeed affected DG. Increasing or decreasing water content at around 41% could increase the gelatinization degree on the extrusion with a four-holed die with a diameter of 2 mm [4]. In addition, the high DG could also be caused by the high amount of amylose leached from starch granules during the gelatinization process [38]. The argument for increasing the DG as desired was to increase the residence time by lowering the screw speed by about 100 rpm.

When the drying process results in sago starch undergoing a slight gelatinization, where the DG of Sago 2 was not significantly higher than other sago. This was possible because it dried using a roasting system for a long time. This can be seen from the darker color of Sago 2, while Sago 1 and 3 were dried using a flash dryer system. The DG of PPSS 1 was not significantly higher than other PPSS. This suggests that Sago 1 was more easily gelatinized. The higher the amorphous, the easier the starch will undergo the gelatinization process because the amorphous area can absorb more water, so the starch granules swell and form a gel [39]. Figure 2 shows Sago 1 as having the smallest crystallinity or largest amorphous area. In addition, Sago 1 has a lower beginning gelatinization temperature (69.9 °C) compared to Sago 2 (71.3 °C) and Sago 3 (74.5 °C) as shown in Table 2.

Sago 1, 2, and 3, which was WSI, also increased significantly when transformed into their PPSS. Likewise, WAI and SP were also increased when the sago was extruded into PPSS. Similarly, WAI and WSI also increased as the moisture content of sago starch increased. Granular integrity was commonly known as the main factor affecting WAI, SP, and WSI [40]. In this study, the sago starch grain surface was smooth without fractures as captured.
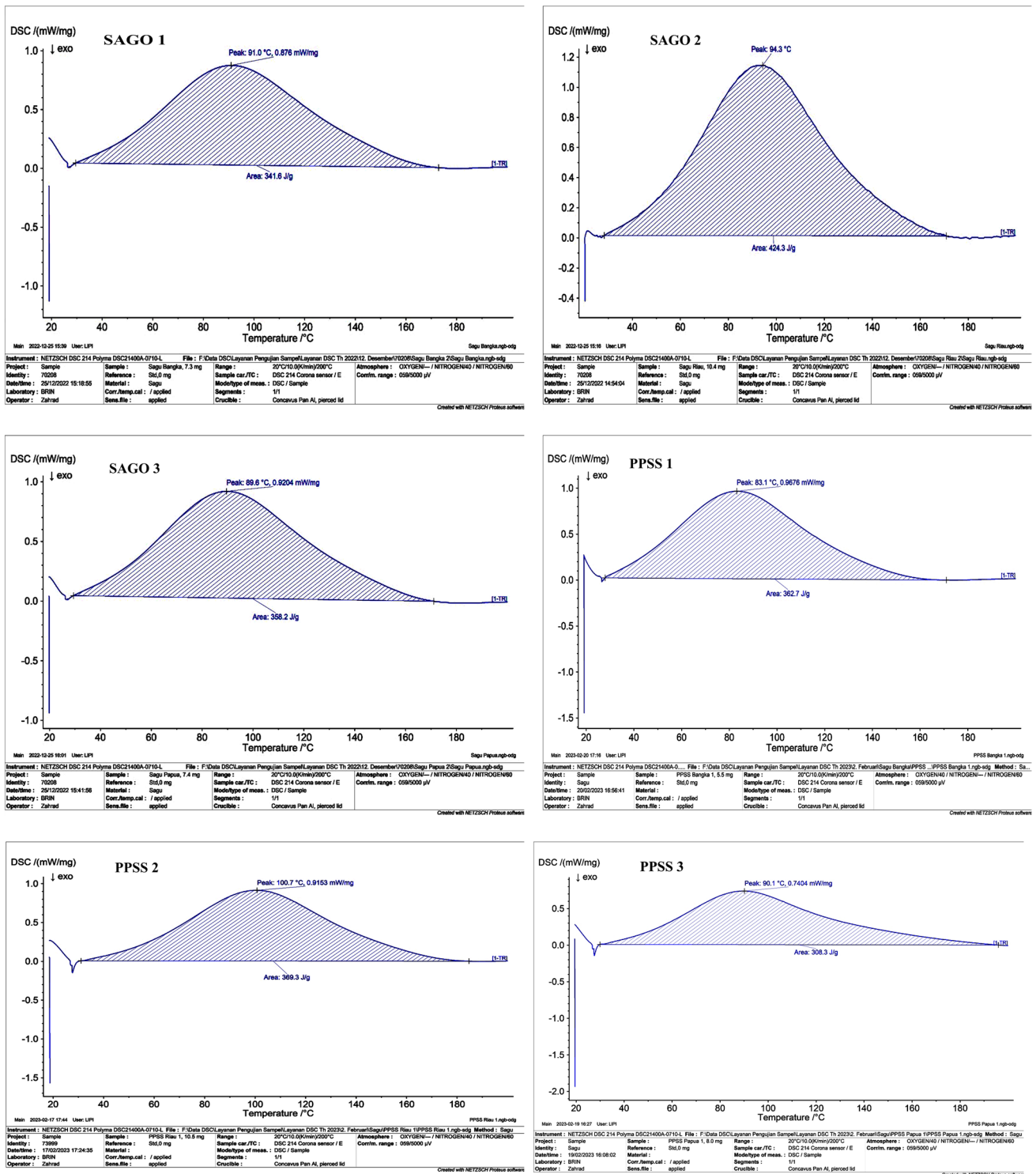
Fig. 4 DSC thermograms of Sago 1, 2, 3, and PPSS 1, 2, 3 samples with a heating rate of 10 °C

In contrast, PPSS has an irregular shape conducive to water infiltrating the starch granules for hydration and leaching. The WSI of PPSS 1 was significantly higher than other PPSS. The WAI of PPSS 1 was considerably higher than PPSS 2 and not significantly higher than PPSS 3. The higher the WSI and WAI were, the better the effect on food processing.

Table 4 pH, BD, DW, viscosity, DG, WSI, WAI, SP, gel properties of Sago 1, 2, 3, and PPSS 1, 2, 3

Starch/extrudate	pH	BD (g/mL)	DW (%)	Viscosity (cP)	DG (%)	WSI (%)	WAI (g/g)	SP (g/g)	Gel strength (g)	Adhesiveness (g.s.)
Sago 1	4.79±0.54[b]	0.756±0.017[ab]	95.24±1.89[f]	0	14.27±6.19[a]	0.128±0.050[b]	2.267±0.046[a]	3.233±0.191[ab]	–	–
PPSS 1	6.52±0.03[d]	0.751±0.002[ab]	91.03±0.28[d]	79	48.91±9.06[b]	0.867±0.050[f]	3.181±0.121[b]	7.470±0.056[d]	37.975±1.177[a]	−3.265±0.495[b]
Sago 2	4.61±0.25[b]	0.781±0.035[bc]	82.16±1.21[b]	0	19.00±11.3[a]	0.296±0.037[d]	2.391±0.054[a]	2.940±0.157[a]	–	–
PPSS 2	6.17±0.02[cd]	0.778±0.029[bc]	64.08±0.94[b]	42	39.82±4.54[b]	0.313±0.054[c]	2.511±0.023[a]	3.710±0.228[b]	3.062±0.965[b]	−8.932±0.343[ab]
Sago 3	3.35±0.11[a]	0.803±0.019[c]	93.07±0.24[e]	0	13.03±0.81[a]	0.050±0.010[a]	2.306±0.091[a]	2.741±0.412[a]	–	–
PPSS 3	5.87±0.01[c]	0.737±0.017[a]	84.82±0.58[c]	40	37.80±12.0[b]	0.574±0.059[e]	3.090±0.329[b]	4.433±0.489[c]	1.663±0.261[b]	−10.699±5.680[a]

Values with the different letters in the same column were significantly different ($p \leq 0.05$)

SP refers to the starch granules' ability to hold water during gelatinization. The SP of the three PPSSs recorded in this paper was higher than that of their respective sago starch. As a result, the three PPSSs tended to have higher granule integrity. In addition, higher SP was probably related to the lower amylose content of the starch. Amylose could inhibit the swelling process as it strengthens the power of connection within the starch granules [41]. SP was also based on amylose and amylopectin bonds, including branching degree, molecular weight distribution, and branch length [42]. SP and WSI of corn starch extrudate were increased as the barrel temperature was increased [43]. The SP of PPSS 1 was significantly higher than PPSS 2 and 3. The higher the SP was, the better the effect on food processing.

Gel properties

The three PPSSs possessed different gel properties because their molecular structure and composition differed (Table 4). In the current study, gel strength and adhesiveness of PPSS 1 were the highest among the three PPSS. The longer amylopectin chain and the higher amount of amylose molecules might partially be responsible for the case. PPSS 1 could form a stronger gel because of a recrystallization process in which disaggregated amylose and amylopectin molecules in gelatinized starches reassociate to form ordered structures [44]. As for the high gel adhesiveness of PPSS 1, syneresis and amylopectin crystallization could be the causes of the phenomenon [45]. Considering these results, PPSS 1 was more suitable for binder production due to its adhesiveness.

Birefringence properties

Birefringence is a property of starch granules that can reflect polarized light so that a light–dark contrast is visible as a blue-yellow color. Liu stated that the birefringence characteristic indicates that the starch granule has a radial orientation of crystallites or a high degree of molecular order within the granule [46]. The loss of birefringence (loss of molecular orientation) properties indicates that the starch has undergone starch granule damage due to extrusion. Figure 5 shows that most of the sago starch granules were oval. The birefringence properties of sago starch were intact, indicated by a light–dark stripe or a clear blue-yellow color on the granules, and the shape was intact. Birefringence was related to the gelatinization point, which was the temperature or gelatinization point at which the birefringence properties of starch begin to disappear [47]. Starch birefringence was lost due to the rupture of starch molecular bonds so that hydrogen bonds could bind more water molecules.

PPSS 1, 2, and 3 found that some of the birefringence properties of granules had been lost. This was because it undergoes partial gelatinization extrusion on PPSS, where
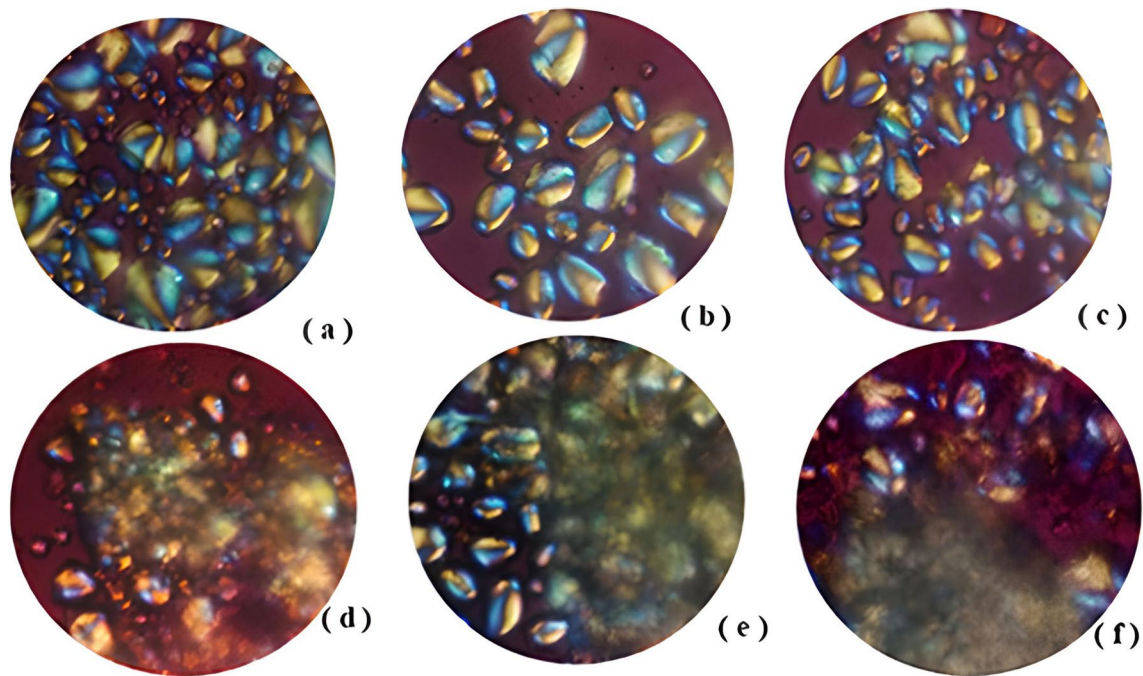
Fig. 5 Birefringence properties of **a** Sago 1, **b** Sago 2, **c** Sago 3, **d** PPSS 1, **e** PPSS 2, and **f** PPSS 3

the extrusion process damages the birefringence properties of the granules. The birefringence properties of starch decrease in proportion to extrusion conditions. This happens because the extrusion process at high water content, temperatures above gelatinization temperature, and high screw speed without die can also damage the birefringence properties of sago.

Conclusion

The extrusion process has changed the physicochemical properties of sago starch. Sago starch from Bangka, Riau, and Papua had their DG increased when extruded into PPSS. This study has shown that the WSI, WAI, SP, and viscosity properties of the three PPSS from the extrusion process have increased while BD and DW have decreased. The crystallinity and enthalpy of PPSS 1 increased after extrusion, while PPSS 2 and 3 decreased. Analysis of gel properties has shown that PPSS 1 has higher gel strength and adhesiveness than PPSS 2 and 3. Analysis of pasting properties has shown that PV Sago 3 and PPSS 3 were much lower than Sago 1 and 2. Birefringence properties of PPSS 1, 2, and 3 have shown that not all were lost; there was still a blue-yellow color. The results of this study showed that extrusion under conditions of 41% moisture content, barrel temperature for zone at 1–4 (40, 81. 81, and 81 °C), respectively, and screw speed at 390 rpm, and without a die at Sago 1, 2, and 3 have produced PPSS 1, 2, and 3 with significantly different

characteristics. All starch can be used as raw material for the production of PPSS. In this study, Bangka sago was chosen for optimization of the extrusion process due to the advantage of its physicochemical characteristics compared to others.

Declarations

References

1. C. Du, F. Jiang, W. Jiang, W. Ge, S. Du, Physicochemical and structural properties of sago starch. Int. J. Biol. Macromol. **164**, 1785–1793 (2020). https://doi.org/10.1016/j.ijbiomac.2020.07.310

2. R.S.A. Rashid, A.M.D. Mohamed, S.N. Achudan, P. Mittis, Physicochemical properties of resistant starch type III from sago starch

at different palm stages. Mater. Today: Proc. (2020). https://doi.org/10.1016/j.matpr.2020.01.511

3. F.F. Hilmi, M.U. Wahit, N.A. Shukri, Z. Ghazali, A.Z. Zanuri, Physico-chemical properties of biodegradable films of polyvinyl alcohol/sago starch for food packaging. Mater. Today: Proc. **16**(4), 1819–1824 (2019). https://doi.org/10.1016/j.matpr.2019.06.056

4. S. Govindasamy, O.H. Campanella, C.G. Oates, High moisture twin-screw extrusion of sago starch: 1. Influence on granule morphology and structure. Carbohydr. Polym. **30**(4), 275–286 (1996). https://doi.org/10.1016/S0144-8617(96)00024-0

5. J.P. Cox, J.M. Cox, Cohesive vegetable product and process for manufacture. US Patent 5252351 (1993)

6. AOAC, *Official Methods of Analysis. Official Method 920.85, 923.03, 925.10, 992.15, 996.11*, 20th edn. (Association of Official Analytical Chemists (AOAC), Rockville, 2016)

7. R. Hoover, W. Ratnayake, *Determination of Total Amylose Content of Starch* (Wiley, Hoboken, 2001)

8. S.J. Mcgrance, H.J. Cornell, C.J. Rix, A simple and rapid colorimetric method for the determination of amylose in starch products. Starch/Stärke **50**(4), 158–163 (1998). https://doi.org/10.1002/(SICI)1521-379X(199804)50:4%3c158::AID-STAR158%3e3.0.CO;2-7

9. J.C. Wang, J.E. Kinsella, Functional properties of novel proteins: alfalfa leaf protein. J. Food Sci. **41**(2), 286–292 (1976). https://doi.org/10.1111/j.1365-2621.1976.tb00602.x

10. M. Wootton, D. Weeden, N. Munk, A rapid method for the estimation of starch gelatinization in processed foods. Food Technol. Aust. **23**, 612–615 (1971)

11. R.A. Anderson, H.F. Conway, V.F. Pfeifer, E.L. Griffin, Gelatinization of corn grits by roll and extrusion cooking. J. Cereal Sci. **14**, 4–12 (1969)

12. H.W. Leach, L.D. Mc Cowen, T.J. Schoch, Structure of the starch granule. I. Swelling and solubility patterns of various starches. Cereal Chem. **36**, 534–544 (1959)

13. W. Wang, W. Chen, H. Yang, M. Cui, Textural and rheological properties of potato starch as affected by amino acids. Int. J. Food Prop. **20**(S3), S3123–S3134 (2017). https://doi.org/10.1080/10942912.2017.1396475

14. M.N. Abdorreza, M. Robal, L.H. Cheng, A.Y. Tajul, A.A. Karim, Physicochemical, thermal, and rheological properties of acid-hydrolyzed sago (*Metroxylon sagu*) starch. LWT **46**, 135–141 (2012). https://doi.org/10.1016/j.lwt.2011.10.015

15. F.B. Ahmad, P.A. Williams, J.L. Doublier, S. Durand, A. Buleon, Physico-chemical characterization of sago starch. Carbohydr. Polym. **38**(4), 361–370 (1999). https://doi.org/10.1016/s0144-8617(98)00123-4

16. J. Park, S.-K. Oh, H.-J. Chung, H.-J. Park, Structural and physicochemical properties of native starches and non-digestible starch residues from Korean rice cultivars with different amylose contents. Food Hydrocoll. **102**, 105544 (2020). https://doi.org/10.1016/j.foodhyd.2019.105544

17. P. Haryanti, R. Setyawati, R. Wicaksono, Effect of temperature and time of heating of starch and butanol concentration on the physicochemical properties of high-amylose tapioca starch. Agritech **34**(3), 308–315 (2014)

18. B. Santoso, K. Sakakura, H. Naito, M. Ohmi, Y. Nishimura, T. Uchiyama, A. Itaya, M. Hisamatsu, H. Ehara, T. Mishima, Effects of micro powder milling on physicochemical properties of sago starch. J. Appl. Glycosci. **62**, 73–80 (2015)

19. S. Sumardiono, B. Jos, I. Pudjihastuti, A.M. Yafiz, M. Rachmasari, H. Cahyono, Physicochemical properties of sago ozone oxidation: the effect of reaction time, acidity, and concentration of starch. Foods **10**, 1309 (2021). https://doi.org/10.3390/foods10061309

20. L.Y. Teng, N.L. Chin, Y.A. Yusof, Rheological and textural studies of fresh and freeze thawed native sago starch-sugar gels. II. Comparisons with other starch sources and reheating effects. Food Hydrocoll. **31**, 156–165 (2013). https://doi.org/10.1016/j.foodhyd.2012.11.002

21. H. Jacobs, J.A. Delcour, Hydrothermal modifications of granular starch, with retention of the granular structure: a review. J. Agric. Food Chem. **46**(8), 2895–2904 (1998). https://doi.org/10.1021/jf980169k

22. C. Loisel, Z. Maache-Rezzoug, C. Esneault, J.L. Doublier, Effect of hydrothermal treatment on the physical and rheological properties of maize starches. J. Food Eng. **73**, 53–64 (2006). https://doi.org/10.1016/j.jfoodeng.2005.01.004

23. M.A.A.H. Allah, H.A.A. Alshamsi, Green synthesis of AC/ZnO nanocomposites for adsorptive removal of organic dyes from aqueous solution. Inorg. Chem. Commun. **157**, 111415 (2023). https://doi.org/10.1016/j.inoche.2023.111415

24. G.K. Mawarni, Rumiyati, T.N.S. Sulaiman, Optimization and characterization of extruded partially pregelatinized cassava starch as filler-binder. Indones. J. Pharm. **34**(1), 79–92 (2023). https://doi.org/10.22146/ijp.5117

25. S. Pérez, E. Bertoft, The molecular structures of starch components and their contribution to the architecture of starch granules: a comprehensive review. Starch/Stärke **62**, 389–420 (2010). https://doi.org/10.1002/star.201000013

26. F. Zhu, Recent advances in modifications and applications of sago starch. Food Hydrocoll. **96**, 412–423 (2019). https://doi.org/10.1016/j.foodhyd.2019.05.035

27. Z. Mokhtari, S.M. Jafari, A.M. Ziaiifar, I. Cacciotti, Extraction, purification, and characterization of amylose from sago and corn: morphological, structural and molecular comparison. Int. J. Biol. Macromol. **255**, 128237 (2024). https://doi.org/10.1016/j.ijbiomac.2023.128237

28. S. Srichuwong, T.C. Sunarti, T. Mishima, N. Isono, M. Hisamatsu, Starches from different botanical sources I: contribution of amylopectin fine structure to thermal properties and enzyme digestibility. Carbohydr. Polym. **60**, 529–538 (2005). https://doi.org/10.1016/j.carbpol.2005.03.004

29. A. Naseri, H. Shekarchizadeh, M. Kadivar, Octenylsuccination of sago starch and investigation of the effect of calcium chloride and ferulic acid on physicochemical and functional properties of the modified starch film. J. Food Process. Preserv. (2019). https://doi.org/10.1111/jfpp.13898

30. A.A. Karim, M.Z. Nadiha, F.K. Chen, Y.P. Phuah, Y.M. Chui, A. Fazilah, Pasting and retrogradation properties of alkali-treated sago (*Metroxylon sagu*) starch. Food Hydrocoll. **22**(6), 1044–1053 (2008). https://doi.org/10.1016/j.foodhyd.2007.05.011

31. Y. Honda, Y. Saito, T. Mishima, N. Katsumi, K. Matsumoto, T. Enomoto, S. Miwa, Characterization of physicochemical and digestive properties of starches from various "dainagon" adzuki beans (*Vigna angularis*) cultivated in Japan. Int. J. Biol. Macromol. **148**, 1021–1028 (2020). https://doi.org/10.1016/j.ijbiomac.2020.01.145

32. T.M. Porter, G.P. Heim, C.P. Kubiak, Effects of electron transfer on the stability of hydrogen bonds. Chem. Sci. **8**, 7324–7329 (2017). https://doi.org/10.1039/c7sc03361c

33. W. Wang, H. Wang, X. Jin, H. Wang, T. Lin, Z. Zhu, Effects of hydrogen bonding on starch granule dissolution, spinnability of starch solution, and properties of electrospun starch fibers. Polymer **153**, 643–652 (2018). https://doi.org/10.1016/j.polymer.2018.08.067

34. Y. Gat, L. Ananthanarayan, Effect of extrusion process parameters and pregelatinized rice flour on physicochemical properties of ready-to-eat expanded snacks. J. Food Sci. Technol. **52**, 2634–2645 (2014). https://doi.org/10.1007/s13197-014-1378-7

35. S.M.M. Duque, I.J.L. Castro, D.M. Flores, Evaluation of antioxidant and nutritional properties of sago (*Metroxylon sagu* Rottb.) and its utilization for direct lactic acid production using

immobilized *Enterococcus faecium* DMF78. Int. Food Res. J. **25**(1), 83–91 (2018)

36. S. Huang, L. Roman, M.M. Martinez, B.M. Bohrer, Modification of physicochemical properties of breadfruit flour using different twin-screw extrusion conditions and its application in soy protein gels. Foods **9**, 1071 (2020). https://doi.org/10.3390/foods9081071

37. Q.B. Ding, A. Paul, T. Gregory, The effect of extrusion conditions on the physicochemical properties and sensory characteristics of rice-based expanded snacks. J. Food Eng. **66**, 283–289 (2005). https://doi.org/10.1016/j.jfoodeng.2004.03.019

38. A. Crowther, The differential survival of native starch during cooking and implications for archaeological analyses: a review. Archaeol. Anthropol. Sci. **4**, 221–235 (2012)

39. P.J. Jenkins, A.M. Donald, Gelatinisation of starch: a combined SAXS/WAXS/DSC and SANS study. Carbohydr. Res. **308**(1–2), 133–147 (1998). https://doi.org/10.1016/S0008-6215(98)00079-2

40. V. Vamadevan, E. Bertoft, Structure-function relationships of starch components. Starch-Stärke **67**(1–2), 55–68 (2015). https://doi.org/10.1002/star.201400188

41. M. Zheng, Q. You, Y. Lin, F. Lan, M. Luo, H. Zeng, B. Zheng, Y. Zhang, Effect of guar gum on the physicochemical properties and in vitro digestibility of lotus seed starch. Food Chem. **272**, 286–291 (2019). https://doi.org/10.1016/j.foodchem.2018.08.029

42. U. Uthumporn, N. Wahidah, A.A. Karim, Physicochemical properties of starch from sago (*Metroxylon sagu*) palm grown in mineral soil at different growth stages. IOP Conf. Ser. Mater. Sci. Eng. **62**, 012026 (2014). https://doi.org/10.1088/1757-899X/62/1/012026

43. Q. Yang, Z. Xiao, Y. Zhao, C. Liu, Y. Xu, J. Bai, Effect of extrusion treatment with different emulsifiers on the thermal stability and structure of corn starch with different emulsifiers. Czech J. Food Sci. **33**, 464–473 (2015). https://doi.org/10.17221/125/2015-CJFS

44. S.G. Ring, P. Colonna, K.J. I'Anson, M.T. Kalichevsky, M.J. Miles, V.J. Morris, P.D. Orford, The gelation and crystallisation of amylopectin. Carbohydr. Res. **162**(2), 277–293 (1987)

45. J. Wang, L. Yu, F. Xie, L. Chen, X. Li, H. Liu, Rheological properties and phase transition of cornstarches with different amylose/amylopectin ratios under shear stress. Starch – Stärke **62**, 667–675 (2010). https://doi.org/10.1002/star.201000059

46. Q. Liu, Understanding starches and their role in foods, in *Food Carbohydrate Chemistry, Physical Properties, and Applications*. ed. by S.W. Cui (CRC Press, Boca Raton, 2005)

47. L.A. Muñoz, F. Pedreschi, A. Leiva, J.M. Aguilera, Loss of birefringence and swelling behavior in native starch granules: microstructural and thermal properties. J. Food Eng. **152**, 65–71 (2015). https://doi.org/10.1016/j.jfoodeng.2014.11.017